Novel Marine Sponge Derived Amino Acids. 8. Conformational Analysis of Jasplakinolide†

Wayne Inman‡ and Phillip Crews*

Contribution from the Department of Chemistry and Institute for Marine Sciences, University of California, Santa Cruz, California 95064. *Received July 7, 1988*

Abstract: An analysis of the solution conformation of jasplakinolide (**1**), a novel macrocyclic ketide cyclodepsipeptide, was completed using NMR data, molecular mechanics, and dynamics calculations. No intramolecular amide hydrogen bonds were observed in **1**. A unique structural feature in **1** resides in the β-tyrosine, where flexibility in the backbone results in two major backbone conformations, i and ii. Thus, the C1-C2-C3-N torsion angle adopts the g^- and g^+ conformations in solution and provides two different orientations of the β-tyrosine phenol side chain. Flexibility was also observed at the side-chain C4-C5-C20-C21 torsion angle, allowing the bromoindole to adopt either C4-C5-C20-C21 a or g^- conformation. The final results, taking into account torsional movement in the backbone and aromatic side chains, revealed four major conformations ia, ig^- and iia, iig^-. Finally, cooperative aromatic ring side-chain coplanar orientations, a molecular tweezer and face-face stacking, were investigated in iig^-. A key feature of our analysis was the measurement of NMR vicinal coupling constants in solvents of low and high dielectric. A good comparison between calculated and measured time-averaged coupling constants was observed in solvents of high dielectric ($\epsilon \approx 35$) and when a large dielectric ($\epsilon > 5R_{ij}$) was incorporated into the calculations. The diastereotropic hydrogens, H2/H′, H10/10′, H14/14′, and H20/20′, were assigned from the relative conformer populations and the calculated and observed coupling constants.

Jasplakinolide (jaspamide, **1**) is a novel bioactive 19-member macrocyclic ketide-cyclodepsipeptide isolated from the marine sponge *Jaspis* sp. We reported the gross structure of **1** (jasplakinolide) based on analysis of two-dimensional NMR data, high-resolution mass spectral results, and information from degradation reactions.[1] Concurrent to our studies were those of Ireland and Faulkner, who in further collaboration with Clardy reported the relative (by X-ray analysis) and absolute stereochemistry (by degradation and chiral HPLC) of **1** (jaspamide).[2] Very recently, Braekman also reported **1** from *Jaspis johnstoni* and found it to be highly ichthytotoxic.[3] Jasplakinolide has potent in vitro cytotoxicity against tumor cells[4] and in vitro and in vivo activity against the fungi *Candida albicans*[5]. Jasplakinolide was the first macrocyclic mixed polyketide depsipeptide[6] reported from a marine organism and has been the subject of total synthesis.[7]

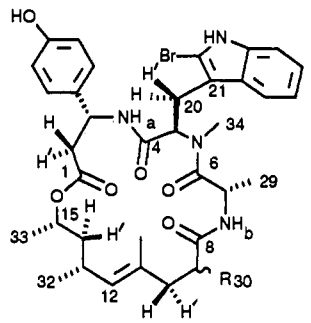

1 R = β CH_3
2 R = α CH_3

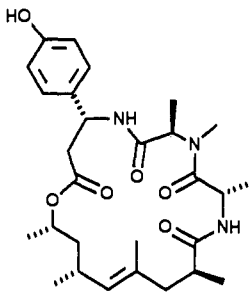

3

We now report on the solution conformation of **1** using NMR, molecular mechanics, and dynamics calculations. The influence of the ususual β-tyrosine on the solution conformation was investigated. In comparison to an α-amino acid, a β-amino acid ($NCHRCH_2CO$) provides a greater potential for flexibility within the peptide backbone due to the possibility of three staggered ethane conformations (g^+, g^-, a) about the N-C-C-C torsion angle. There are only two reported studies on the conformation of β-amino acids. One report on synthetic cyclotri-β-alanyl indicated the macrocycle was flexible, having 12 conformations within an energy difference of 3.9 kcal/mol.[8] By contrast, a rigid conformation was determined for iturin A, a family of cyclic octapeptides composed of α-amino acids and a single β-amino acid having a lipophilic side chain.[9]

The combination of NMR analysis with molecular dynamics and mechanics calculations[10] provides a powerful tool to study the conformations of complex molecules in solution. One approach, effective when a single rigid conformation dominates, utilizes quantitative NOESY data[11] as constraints in molecular dynamics calculations.[12] Alternatively, the analysis of molecules with flexible conformations[13] is important because many biomo-

† First presented at the 1987 American Chemical Society Pacific Conference on Chemistry and Spectroscopy, Irvine, CA, October 28, 1987; Abstract 24.

‡ UC Sea Grant Trainee Fellow, 1987-1989.

(1) Crews, P.; Manes, L. V.; Boehler, M. *Tetrahedron Lett.* **1986**, *27*, 2797.
(2) Zabriskie, T. M.; Klocke, J. A.; Ireland, C. M.; Marcus, A. H.; Molinski, T. F.; Faulkner, D. J.; Xu, C.; Clardy, J. C. *J. Am. Chem. Soc.* **1986**, *108*, 3123.
(3) Braekman, J. C.; Daloze, D.; Moussiaux, B. *J. Nat. Prod.* **1987**, *50*, 994.
(4) Cytotoxicity data: P388 IC_{50} = 0.01 μg/mL (data for HBSP) or 0.04 μg/mL (data from NCI) (vs chemotherapeutic standards, fluorouracil IC_{50} = 0.04 μg/mL and methotrexate IC_{50} = 0.04 μg/mL) and KB IC_{50} = 0.1 μg/mL. At the NCI jasplakinolide (NSC no. 613009) has proven to be active in vitro against 36 human solid tumor cell cultures.
(5) It has been recently shown that *C. albicans* treated with **1** (25 μg/mL) undergoes a reduced rate of [^{3}H]thymidine incorporation, which implies a suppressed rate of DNA synthesis: Scott, V. R.; Boehme, R.; Matthews, T. R. *Antimicrob. Agents Chemother.*, in press.
(6) The geodiamolides represent additional new examples. Isolation: Chan, W. R.; Tinto, W. F.; Manchand, P. S.; Todaro, L. J. *J. Org. Chem.* **1987**, *52*, 3091. Synthesis: Grieco, P. A.; Perez-Medrano, A. *Tetrahedron Lett.* **1988**, *29*, 4225.
(7) (a) Grieco, P. A.; Hon, Y.-S.; Perez-Medrano, A. *J. Am. Chem. Soc.* **1988**, *110*, 1630. (b) Schmidt, U.; Siegel, W.; Mundinger, K. *Tetrahedron Lett.* **1988**, *28*, 1269.
(8) (a) White, D. N. J.; Morrow, C.; Cox, P. J.; Drey, C. N. C.; Lowbridge, J. *J. Chem. Soc., Perkin Trans. 2* **1982**, 239. (b) Lowbridge, J.; Mtetwa, E.; Ridge, R. J. Drey, C. N. C. *J. Chem. Soc., Perkin Trans.* **1986**, 155.
(9) Marison, D.; Genest, M.; Caille, A.; Peypoux, F.; Michel, G. *Biopolymers* **1986**, *25*, 154.
(10) For recent examples, see: (a) Kessler, H.; Bats, J. W.; Griesinger, C.; Koll, S.; Will, M.; Wagner, K. *J. Am. Chem. Soc.* **1988**, *110*, 1033. (b) Hruby, V. J.; Kao, L.-F.; Pettitt, B. M.; Karplus, M. *J. Am. Chem. Soc.* **1988**, *110*, 3351.
(11) Recent examples of this approach are: (a) Fesik, S. W.; Bolis, G.; Sham, H. L.; Olejniczak, E. T. *Biochemistry* **1987**, *26*, 1851. (b) Wüthrich, K. *NMR of Proteins and Nucleic Acids*; Wiley: New York, 1986; 262. (c) Suauki, E.; Pattabiraman, N.; Zon, G.; James, T. L. *Biochemistry* **1986**, *25*, 6854. (d) Olejniczak, E. T.; Gampe, R. T., Jr.; Fesik, S. W. *J. Magn. Reson.* **1986**, *67*, 28. (e) Masseski, W., Jr.; Bolton, P. H. *J. Magn. Reson.* **1985**, *65*, 526. (f) Bax, A.; Davis, D. G. *J. Magn. Reson.* **1985**, *63*, 207.
(12) For a comment on the problems in applying quantitative NOESY data to conformationally mobile biomolecules, see: Kessler, H.; Griesinger, C.; Lautz, J.; Müller, A.; van Gunsteren, W. F.; Berendsen, H. J. C. *J. Am. Chem. Soc.* **1988**, *110*, 3393.

0002-7863/89/1511-2822$01.50/0

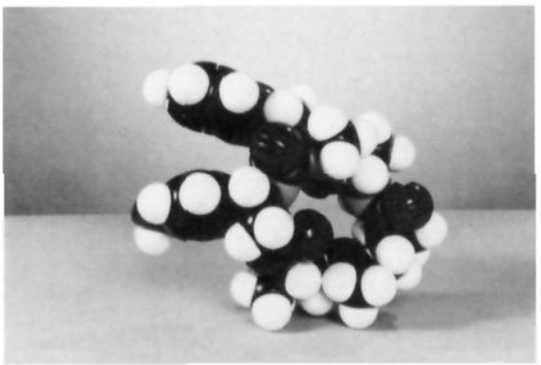

Figure 1. CPK model of **1** showing the aromatic side chains in a parallel-like or tweezer arrangment.

lecules of current interest, such as cyclic[12,10b] and linear[14] peptides, may not be rigid in solution. The conformational study of a flexible peptide must consider torsional movement within the backbone and side chains, the influence of the side chains on the preferred backbone conformations, and cooperative effects between multiple side chains. There is also the possibility that certain side-chain orientations may impart a specific overall molecular shape and biological activity.[10,15] For example, a CPK model of **1** (Figure 1) indicates that the phenol and indole side chains may adopt a molecular tweezer[16] conformation where the two coplanar aromatic rings are approximately 7 Å apart, but specific conformational restrictions on the macrocycle are required for this to occur. Determination of the overall molecular topography of **1** seemed especially relevant because its biological activity may vary as a function of conformational changes. For example, the insect antifeedant properties of **1** and 9-epimethyljasplakinolide (**2**) apparently differ,[17] and proton NMR analysis of **2** in CD_3OD indicated a different conformation about the C1–C2–C3–N torsion angle in comparison to **1**.

Experimental Section

Source of Compounds. Jasplakinolide (**1**) was isolated as previously described,[1,2] and **2** was a generous gift from Prof. Paul Grieco (University of Indiana).

NMR. NMR spectra were recorded at 20 °C on a GN-300 NMR spectrometer, and NH and OH temperature dependencies were measured in DMSO-d_6 over a temperature range of 20–100 °C. The ^1H and ^{13}C chemical shifts of **1** were previously assigned by analysis of COSY experiments in $CDCl_3$ and DMSO-d_6.[1,2] A 49 mM solution of **1** in DMSO-d_6/D_2O (75/25 volume ratio) was used in NOESY experiments with a $(90\text{-}t_1\text{-}90\text{-}\tau_m\text{-}90\text{-acquire})_n$ pulse-sequence and phase-cycling scheme designed to separate the real and imaginary parts of the t_1 dimension.[18] Three NOESY data sets (256 × 1 K) were collected with mixing times (τ_m) of 100, 250, and 600 ms using a delay of 3.0 s between scans. Only the NOESY correlations observed at all three mixing times were reported (Table II). Spectral simulations of chemical shifts and coupling constants were calculated by best fit to peak positions with GEMSIM.

Computational Methods. Computer modeling was carried out with the MACROMODEL program (version 1.5) on a Vax 11/750 computer with an Evans and Sutherland (PS 330) picture system. Initial calculations started with coordinates reported for the X-ray structure of the acetate derivatives of **1**.[19] Molecular mechanics and dynamics calculations were performed with the Amber force field with a distance-dependent dielectric, $\epsilon = R_{ij}$.[20] Solvation effects were approximated by increasing the distance dependence, $\epsilon > R_{ij}$. Constrained minimizations and dynamics were calculated with an extra harmonic term of the form $k(\theta - \theta_0)$ added to the force field. Structures were energy minimized with the Block Diagonal Newton Raphson algorithm in Cartesian coordinate space until the rms energy gradient was less than 0.04 kJ/mol Å. Vicinal coupling constants (^3J) in the candidate conformations were calculated in MACROMODEL with the appropriate coupling equation for peptide,[21] allylic,[22] and aliphatic[23] dihedral angles.

Potential solution-phase conformations were generated by three general methods described below. Exceedingly long computational time was required for energy minimization of **1** due to side-chain interactions. Alternatively, calculation times were substantially reduced in the hypothetical compound **3**.

Method 1 (Dynamics). There are two approaches that increase conformational interconversions during dynamics restricted to a short time period. Calculations at higher temperatures are one obvious approach. By contrast, an increase in the dielectric reduces electrostatic interactions between polar groups and increases conformational interconversions. Molecular dynamics at three temperatures (300, 500, and 600 K) with 1.0-fs time steps for a total of 10–30 ps were calculated with $\epsilon = R_{ij}$. Structures were sampled by time at 0.2-ps intervals. The sampled structures from the dynamics trajectories were then energy minimized.

Method 2 (Multiconformer Search). A multiconformer search was carried out using the MULTICONF routine in MACROMODEL. This search was on **3** and used constraints derived from NMR data of **1** to generate reasonable candidate conformations. Torsion angle constraints for selected angles H3–H_a, H_b–H7, H9–H10, H9–H10′, and H12–H13 were derived from ^3J data. Amide and ester bonds were constrained in the trans geometry. The remaining 10 torsion angles were sampled at 60° intervals. Approximate distance constraints (2–4 Å) were imposed from the observed intense NOESY correlations between H7–Me34, Me29–Me34, H9–H12, and H13–Me31. NOESY correlations were not used quantitatively to estimate interproton distances because conformational mobility in certain parts of the macrocycle result in unrepresentative time-averaged distances. The closure bond was chosen at C14–C15 with a closure limit of 1–3 Å. A total of 200 starting point structures were generated with the above criteria. The starting point structures were minimized and 13 unique structures within 50 kJ/mol of the lowest energy conformer were calculated.

Method 3 (Interactive Model Building). Potential solution-phase conformations that were not obtained by method 1 or 2 were generated by interactive model building (dihedral driving) using constrained minimization.

Table I. Temperature ($d\delta/dT$ in DMSO) and Solvent ($\Delta\delta$) Dependence of NH Amide, and NH/OH Aromatic Chemical Shifts

	$-\Delta\delta/\Delta T \times 10^{-3}$ [a]	$\Delta\delta = \delta_{DMSO} - \delta_{CDCl_3}$ [b]
NH_a	6.88	0.73
NH_b	4.27	1.10
NH_c	3.64	2.60
OH	4.94	1.74

[a] ppm/°C. [b] ppm.

Table II. NOESY Correlations Observed in **1** (DMSO-d_6/D_2O)

H13–Me31	Me29–Me34	H7–Me34	H9–H12	H3–H17	H5–H23

Results and Discussion

The conformational analysis of **1** was begun with a model based on the coordinates of the X-ray structure.[19] However, the solid-state geometry did not agree with our preliminary deduction of the solution conformation based on the existing NMR data. Further work to resolve this discrepancy invovled (1) mechanics calculations of all accessible solution conformations and subsequent

(13) For recent examples dealing with a flexible system, see: (a) Colucci, W. J.; Gandour, R. D.; Mooberry, E. A. *J. Am. Chem. Soc.* **1986**, *108*, 7141. (b) Raap, J.; van Boom, J. H.; van Lieshout, H. C.; Haasnoot, C. A. G. *J. Am. Chem. Soc.* **1988**, *110*, 2736. (c) Reference 11 and references within these.

(14) For a recent example, see: Podanyi, B.; Reid, R. S. *J. Am. Chem. Soc* **1988**, *110*, 3805.

(15) Cheung, H. T.; Feeney, J.; Roberts, G. C.; Williams, D. H.; Ughetto, G.; Waring, M. J. *J. Am. Chem. Soc.* **1978**, 100, 46.

(16) This term was coined by: Chen, C.-W.; Whitlock, H. W. *J. Am. Chem. Soc.* **1978**, *100*, 4921.

(17) Unpublished results from Prof. Paul Grieco (University of Indiana). Compound **2** was obtained during Grieco's total synthesis of jasplakinolide (ref 7a).

(18) Pulse sequence taken from GE GN-300 software manual.

(19) The X-ray coordinates, kindly supplied by Prof. J. Clardy (see ref 2), were used in the model building.

(20) Weiner, S. J.; Kollman, P. A.; Case, D. A.; Singh, U. C.; Ghio, C.; Alagona, G.; Profeta, S.; Weiner, P. *J. Am. Chem. Soc.* **1984**, *106*, 765.

(21) Pardi, A.; Billeter, M.; Wüthrich, K. *J. Mol. Biol.* **1984**, *180*, 741.

(22) Garbisch, E. W. *J. Am. Chem. Soc.* **1964**, *86*, 5561.

(23) Haasnoot, C. A. G.; De Leeuw, F. A. A. M.; Altona, C. *Tetrahedron* **1980**, *36*, 2783. The estimated precision (root-mean-square deviation) of the calculated coupling constant equation was 0.48 Hz.

Table III. Diastereotopic ^1H Chemical Shifts (δ) and Differences ($\Delta\delta$)

solvent	2/2′	10/10′	14/14′	20/20′
$CDCl_3$	2.65/2.63 (0.02)	2.39/1.89 (0.50)	1.30/1.12 (0.18)	3.36/3.22 (0.14)
CD_3CN	2.68/2.60 (0.08)	2.19/1.87 (0.32)	1.41/1.13 (0.28)	3.23/3.10 (0.13)
DMSO-d_6	2.90/2.85 (0.05)	2.32/2.00 (0.32)	1.73/1.48 (0.25)	*a*

[a] Not observable.

Table IV. Observed Coupling Constants ($^3J_{obsd}$ ± 0.3 Hz)

	^3J, Hz			
	$CDCl_3$	CD_3CN	DMSO-d_6	CD_3OD
H2–H3	4.5	4.0	4.2	4.1
H2′–H3	5.7	7.1	9.0	8.0
NH_a–H3	8.7	8.4	8.7	8.7
NH_b–H7	6.9	6.9	7.5	7.2
H9–H10	11.1	11.4	9.9	11.7
H9–H10′ [a]	<2.5	<2.5	<2.5	<2.5
H12–H13	10	9.0	9.0	*b*
H13–H14	11.7	8.8	*b*	10.2
H13–H14′	*b*	5.4	5.7	4.8
H14–H15	3.0	6.0	*b*	5.8
H14′–H15	*b*	7.8	6.3	8.2
H5–H20	6.6	6.1	*b*	7.2
H5–H20′	10.2	10.1	*b*	9.3

[a] A coupling of 2.7 Hz was measured at 60 °C in DMSO-d_6. Below this temperature no coupling was measurable due to the broad absorption of H10′; therefore, the H9–H10′ coupling value is reported as <2.5 Hz. [b] Not observable.

evaluation of them using NMR data and (2) the measurement of additional NMR parameters in different solvents to probe conformational homogeneity.[24]

The first goal of the conformational search was to determine probable macrocycle backbone conformations in **3**, while ignoring effects from the bromoindole side chain in **1**. All possible staggered ethane conformations about the four key torsion angles, C1–C2–C3–N, C8–C9–C10–C11, C12–C13–C14–C15, and C13–C14–C15–O, were generated (Experimental Section, methods 1–3). Relative conformer populations were then determined by a Boltzmann distribution based on their minimized energies.[13a] Time-averaged NMR vicinal proton coupling constants were calculated from the relative populations. These were compared to experimental values determined in various solvents which included exact vicinal coupling constants, diastereotopic ^1H chemical shift differences, NOESY correlations, and amide proton temperature coefficients. To fully test for conformational homogeneity, NMR data were obtained in four different solvent types (Table I–IV). Finally, the calculated time-averaged coupling constants were compared to experimental values and six low-energy conformations, i–vi (Table V), were eventually identified by this process.

Intramolecular Hydrogen Bonding. Distinct conformational restriction often occurs in cyclic pentapeptides and hexapeptides comprised entirely of α-amino acids owing to intramolecular amide hydrogen bonds.[25] Only scant data exist about intramolecular H bonding in cyclopeptides containing either all β-amino acids[8] or a mixture of α- and β-amino acids.[9,26] In **1**, both H_a and H_b exhibit temperature[25,27] and solvent dependence,[25,28] summarized in Table I, in the range expected when no intramolecular hydrogen bond exists in solution.

Amide and Ester (ω) Torsion Angles. The amides C3–N–C4–C5, C5–N–C6–C7, C7–N–C8–C9, and ester C15–O–C1–C2 bonds were initially configured in the trans geometry, as also found in the solid-state conformation.[2,19] There was reasonable doubt about the lowest energy geometry about the C5–N(Me)–C6–C7 amide torsion angle due to amide cis,trans isomerization. This point was investigated by D NMR, and no isomerization was observed from −20 to 150 °C. An extensive multiconformer search predicted the global minimum with a trans C5–N–C6–C7 amide. Furthermore, only the trans C5–N–C6–C7 amide is consistent with the intense NOESY correlations observed between H7–Me34 and Me29–Me34 (Table II).

Substituted Ethane Torsion Angles. A substituted ethane having the general formula $R_1R_2HCCH_2R_3$ may adopt three staggered conformations, g^-, g^+, or a, as shown in the generalized conformations below.[29] There are 81 possible conformations for the

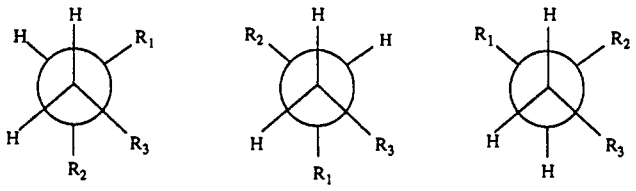

Generalized Conformations

four ethane subunits, C1–C2–C3–N, C8–C9–C10–C11, C12–C13–C14–C15, and C13–C14–C15–O, assuming 120° rotation increments between staggered conformations.[30] The macrocycle of **1** is large enough for the ring atoms to occupy anti positions (e.g., R_2/R_3 or R_1/R_3 above), yet the cyclic constraint also limits the inherent flexibility of the backbone.

The analysis of staggered ethane conformations involved consideration of two cases. *Case 1* involved a rigid ethane fragment. The two vicinal couplings may be used to differentiate between g^- and g^+/a. The vicinal proton coupling constants for g^- are approximately 3 Hz, whereas g^+ and a have divergent values, approximately 3 and 12 Hz. It is more difficult to distinguish between g^+ and a, and the final analysis must involve making specific assignments for the diastereotopic protons, H and H′. As will be shown later, one effective strategy involves calculating minimized energies for g^+ and a that can then be used to determine which conformer predominates. Additional evidence was attained with NOESY measurements to reveal a specific spatial relationship of some group of H or H′. *Case 2* involves flexible ethane torsion angles where the solution conformation represents a time-averaged structure. Estimates of the relative populations of g^-, g^+, and a can be made by a Boltzmann distribution using energies obtained from molecular mechanics calculations.[13] Prochirality of the diastereotopic hydrogens may then be assigned by analysis of the relative conformer populations, the calculated and the observed vicinal coupling constants.

Rigid and flexible torsion angles of substituted ethanes may be identified by comparing NMR measurements with molecular

(24) Conformational homogeneity is defined as one set of NMR signals corresponding to one molecular conformation; see: reference 12.

(25) For key literature, see: (a) Kessler, H. *Angew Chem., Int. Ed. Engl.* **1982**, *21*, 512. (b) Govil, G.; Hosur, R. V. *Conformation of Biological Molecules, New Results from NMR*; Springer-Verlag: New York, 1982; pp 116–119.

(26) Naturally occurring cyclic peptides with a mixture of α- and β-amino acids are extremely rare, the only examples being jasplakinolide,[1,2] the iturins,[9] and cyanogenosin-RR (Painuly, P.; Perez, R.; Fukai, T.; Shimizu, Y. *Tetrahedron* **1988**, *29*, 11.

(27) Kopple, K. D.; Ohnishi, M.; Go, A. *J. Am. Chem. Soc.* **1969**, *91*, 4264.

(28) Stezowski, J. J.; Pohlmann, H. W.; Haslinger, E.; Kalchauser, H.; Schmidt, U.; Pozolli, *Tetrahedron* **1987**, *43*, 3923.

(29) The $g^+/g^-/a$ nomenclature describes the general dihedral angular relationship of any carbon–carbon chain backbone. The assignment requires that a priority be established for the R groups (e.g., $R_1 > R_2$, and the front carbon of the Newman projection is arbitrarily of higher priority). The $g^+/g^-/a$ nomenclature is not general but depends on the *R/S* stereochemistry at the chiral carbon of the ethane backbone (e.g., a switch of R_1/R_2 in the generalized g^+ conformer, shown in the text, results in an a conformation).

(30) Number of possible conformations = $(360°/\blacktriangle)^n$, where ▲ is the rotational increment angle (e.g., 120°) and *n* is the number of bonds about which rotation occurs (e.g., four).

Table V. Summary of Conformers for **3**: Energies, Populations, and Torsion Angles from Molecular Mechanics Calculations ($\epsilon = 5R_{ij}$)

	conformer						
	i	ii	iii	iv	v	vi	X-ray[a]
rel energy,[b] kJ/mol	0.0	0.5	3.9	4.2	5.5	6.8	
population	0.42	0.34	0.09	0.08	0.05	0.03	
ethane notation[c]	$g^-g^+g^-a$	$g^+g^+g^-a$	$g^+g^+g^-g^+$	$g^+g^+g^+g^+$	$g^-g^+g^+g^+$	$g^+g^+ag^+$	$g^-g^+g^-a$
			Ethane Torsion Angles, deg				
C1–C2–C3–N	298.5	50.7	60.7	52.6	303.6	61.7	295.9
C8–C9–C10–C11	57.0	70.4	64.6	55.5	55.9	74.9	81.2
C12–C13–C14–C15	294.3	284.5	289.3	44.4	47.4	184.9	296.6
C13–C14–C15–O	169.1	155.7	89.8	70.4	70.0	49.3	168.6
			φ Torsion Angles, deg				
C2–C3–N–C4	292.0	241.8	264.6	201.8	295.9	183.0	212.8
C6–C7–N–C8	198.0	199.8	203.4	197.7	205.4	223.4	202.0
C4–C5–N–C6	87.6	90.4	88.5	84.2	84.8	90.3	110.5
			ω Torsion Angles, deg				
C3–N–C4–C5	171.6	175.4	170.3	175.6	171.9	182.0	187.1
C5–N–C6–C7	181.6	169.9	187.3	182.3	187.3	174.2	182.0
C7–N–C8–C9	179.2	188.9	183.0	176.1	179.5	181.7	192.7
C15–O–C1–C2	176.6	180.1	192.0	189.9	184.2	181.0	176.0
			ψ Torsion Angles, deg				
N–C4–C5–N	299.4	289.4	294.4	288.7	298.8	268.0	336.0
N–C6–C7–N	166.7	91.7	85.7	162.6	161.1	86.3	157.4
			Other Torsion Angles, deg				
O–C1–C2–C3	263.4	55.7	86.2	66.8	244.0	113.3	245.6
N–C8–C9–C10	198.7	230.1	219.5	208.7	196.9	288.1	219.9
C9–C10–C11–C12	60.4	79.6	85.7	61.7	44.2	76.8	346.0
C14–C15–O–C1	200.6	268.5	253.0	238.5	195.3	64.8	275.1
C11–C12–C13–C14	126.4	117.2	151.2	66.8	68.2	102.6	138.6
C10–C11–C12–C13	176.7	178.3	170.2	182.5	172.9	181.5	179.7

[a] Torsion angles reported for the acetate derivative of **1**.[2] [b] 4.18 kJ = 1 kcal. [c] The $g^+/g^-/a$ nomenclature is used to describe the torsion angles about the substituted ethanes C1–C2–C3–N, C8–C9–C10–C11, C12–C13–C14–C15, and C13–C14–C15–O, respectively.

dynamics and mechanics calculations. Small chemical shift differences (≈0.1 ppm) between diastereotopic protons are typically interpreted to indicate flexibility at that site,[31] and such a conclusion is strengthened by also considering the pattern of vicinal couplings to the diastereotopic hydrogens. The diastereotopic ^1H chemical shift differences for H2–H2′, H10–H10′, and H14–H14′ and the vicinal coupling constants (^3J) are reported in Tables III and IV.

C1–C2–C3–N Torsion Angle. The small diastereotopic shift difference between H2 and H2′ [0.08 ppm (CD_3CN)] and the intermediate ^3J values for H2–H3 [4.0 Hz (CD_3CN)] and H2′–H3 [7.1 Hz (CD_3CN)] suggest that the C1–C2–C3–N torsion angle within the β-amino acid is flexible and represents an average of several staggered conformers shown below. Also consistent with the NMR results was the conversion of the g^- to the g^+ state during a 10-ps dynamics trajectory at 600 K. Two trajectories at 300 and 600 K are shown in Figure 2. Minimization of generated structures revealed that g^- and g^+ but not a are low-energy conformations about the C1–C2–C3–N angle.

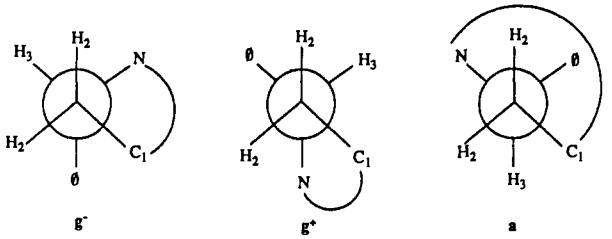

[C_1-C_2-C_3-N Conformations]

C8–C9–C10–C11 Torsion Angle. The relatively large diastereotopic shift difference between H10 and H10′ [0.50 ppm ($CDCl_3$)] along with the extreme difference in ^3J values for H9–H10 (11.1 Hz) and H9–H10′ (<2.5 Hz) indicates that the C8–C9–C10–C11 torsion angle is rigid. The J values imply the torsion angle is locked into either the g^+ or a conformation shown below. The g^+ conformation is consistent with the intense NOESY correlation between H9–H12 (see Figure 3). Results from dynamics and mechanics calculations consistently predicted the g^+ conformer to have a substantially lower energy than the a.

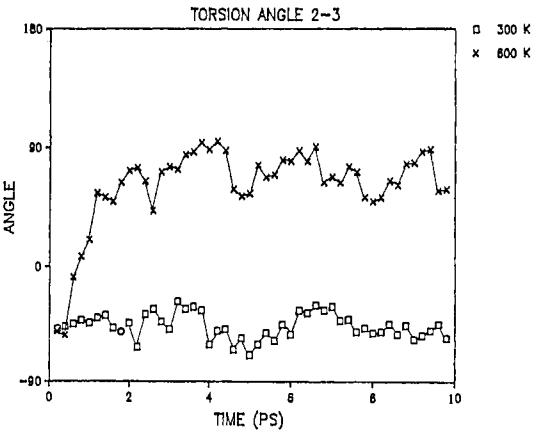

Figure 2. Molecular dynamics trajectories of **1** showing changes in the torsion angle C1–C2–C3–N as a function of time at 300 and 600 K.

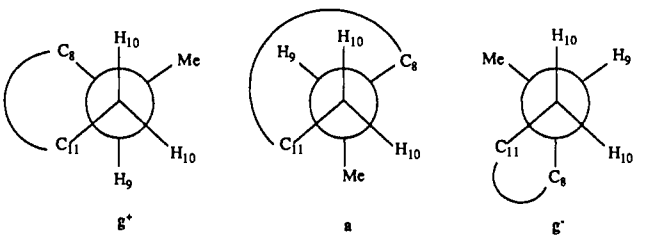

[C_8-C_9-C_{10}-C_{11} Conformations]

C12–C13–C14–C15 Torsion Angle. The ^3J values for H13–H14 are solvent dependent and demonstrate the torsion angle is not

(31) (a) Reference 10b. (b) Reference 25a.

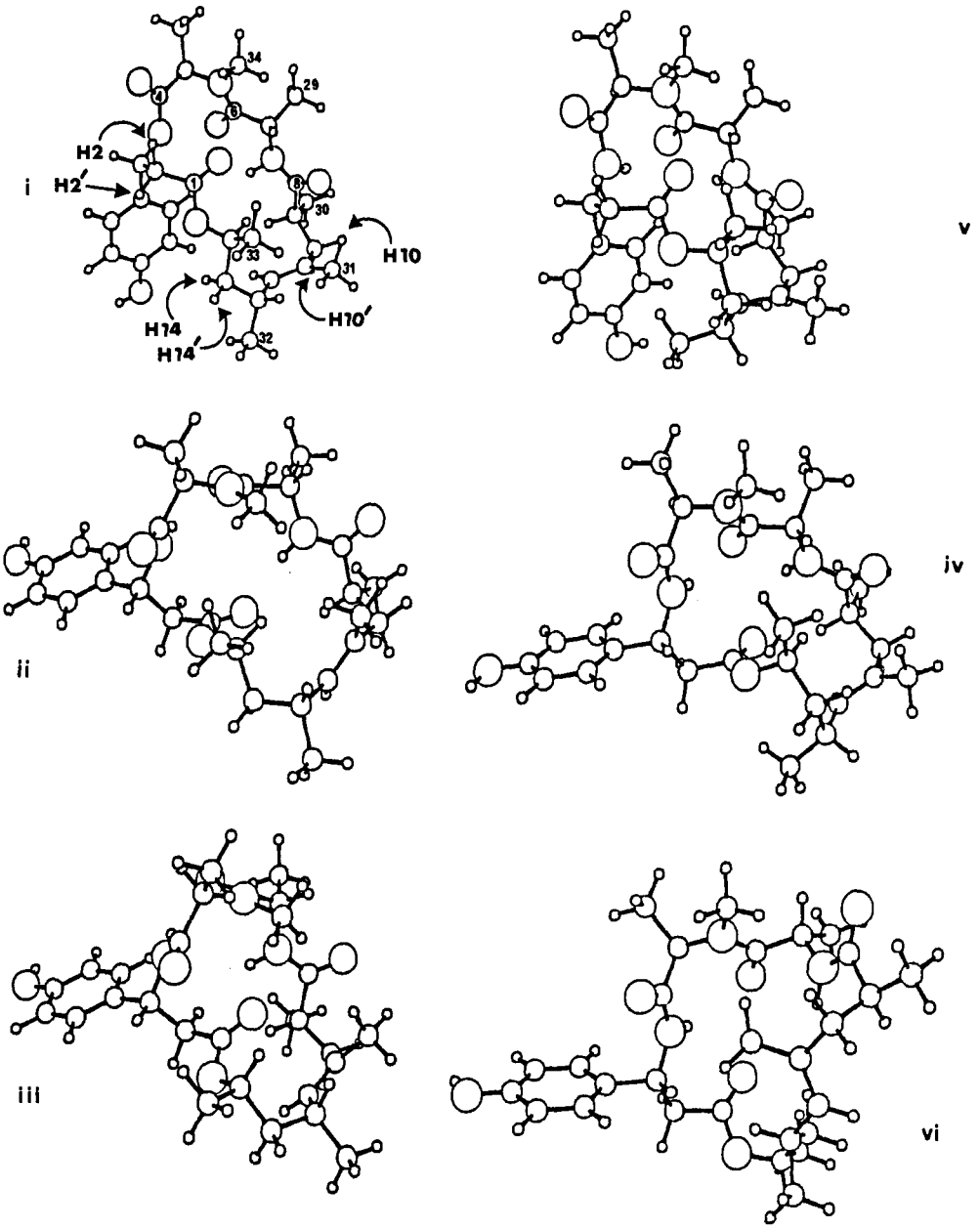

Figure 3. ORTEP plots of conformers i–vi.

conformationally homogeneous. The coupling constant values in polar solvents for H13–H14 [8.8 Hz (CD_3CN), 10.2 Hz (CD_3OD)] and H13–H14′ [5.4 Hz (CD_3CN), 4.8 Hz (CD_3OD)] suggest the C12–C13–C14–C15 torsion angle is predominantly

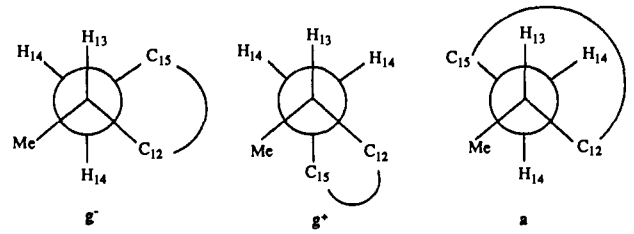

either g^- or a with a possible contribution from the g^+ conformation shown below. Modeling results predict the torsion angle is predominantly g^- with minor contributions from g^+. An intense NOESY correlation between H13–Me31 is consistent with the g^- conformation (Figure 3).

C13–C14–C15–O Torsion Angle. The ^3J values for H14–H15 change dramatically between nonpolar and polar solvents, and similar coupling constants for H14–H15 [6.0 Hz (CD_3CN)] and H14′–H15 [7.8 Hz (CD_3CN)] indicate this torsion angle is flexible. The ^3J values for H14–H15 and H14′–H15 are time-averaged values of several conformers. Modeling calculations predicted the torsion angle to be composed of both the a and g^+ conformers shown below.

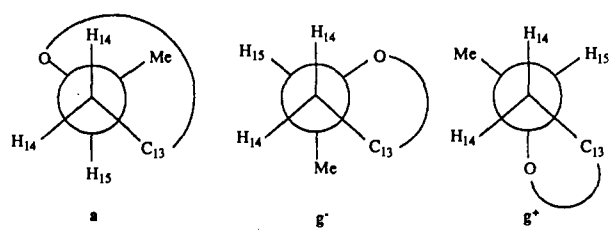

Backbone Conformation. On the basis of minimization energies, only 6 of the possible 81 macrocycle conformations of **3** (i–vi) are predicted to contribute to the conformational equilibrium. Conformers i–vi are shown in Figure 3, and torsion angles are listed in Table V. On the basis of the g^- or g^+ torsion angle about C1–C2–C3–N, these conformers may be grouped into two families

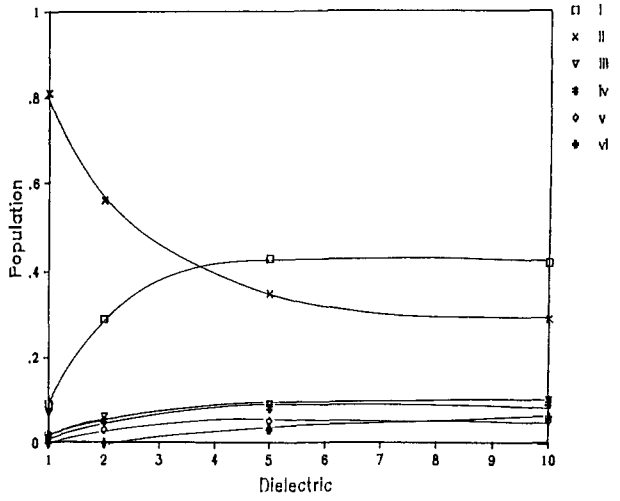

Figure 4. Relative i–vi conformer populations predicted by molecular mechanics as a function of the distance-dependent dielectric ($\epsilon = nR_{ij}$).

composed of i, v, and ii, iii, iv, vi, respectively. The two major conformers, i and ii, differ by a 120° rotation at the C1–C2–C3–N torsion angle and represent each of the two families noted above. Conformer i is similar to the solid-state conformation of **1** (Table V) and suggests it is valid to examine the overall backbone conformation of jasplakinolide independent of the aromatic substitutuents. The minor conformers of two families above may be compared in terms of the torsion angles about C12–C13–C14–C15 and C13–C14–C15–O. Thus, the difference between i and v (both are in the same family) involves approximate 120° rotations at both the C12–C13–C14–C15 and C13–C14–C15–O torsion angles. Similarly, differences between ii and the other members of its family including iii, iv, vi are as follows. Conformers ii and iii differ by a 120° rotation at the C12–C13–C14–C15 torsion angle, whereas ii differs from iv and vi by 120° rotations at both the C12–C13–C14–C15 and C13–C14–C15–O angles.

The relative conformer populations of i–vi were determined by a Boltzmann distribution using the minimized energies. The relative energies of i–vi were dependent on the dielectric constant used in the force field and represent the influence of solvation. The electrostatic energy term in the force field is given in eq 1,

$$E_{el} = q_i q_j / \epsilon R_{ij} \quad (1)$$

where the distance-dependent dielectric (ϵ) equals R_{ij}.[17] Solvation effects were approximated by increasing the distance-dependent dielectric, $\epsilon > R_{ij}$. Previous studies have shown a dependence of the minimized energy and relative conformer populations on the dielectric with polar groups such as organic halides,[32] nucleosides,[20] or zwitterions.[13a] A distance-dependent dielectric of $\epsilon = 4R_{ij}$ was required to reproduce the relative C2′ endo/C3′ endo energy in adenosine.[20] Overemphasized electrostatic interactions in a cyclic hexapeptide were noted in molecular dynamics calculations with a dielectric of 1.0.[10a] Electrostatics were found to be a dominant factor in determining the relative energies/populations of conformers i–vi with values of $\epsilon < 5R_{ij}$. A crossover in the relative populations of the major conformers, i and ii, occurred with values of $\epsilon < 5R_{ij}$ and is shown in Figure 4. Conformer ii becomes dominant (81%) at $\epsilon = R_{ij}$ due to *transannular* electrostatic interactions. Models of ii show the carbonyl group at C1 is positioned inside the ring with the negative-charged oxygen in close proximity to the positive-charged amide H_b and C8 atoms. The largest difference in electrostatic energy (−7.5 kJ/mol) between ii and i was calculated at $\epsilon = R_{ij}$, whereas a small difference (−0.9 kJ/mol) was observed at $\epsilon = 5R_{ij}$. With $\epsilon < 5R_{ij}$ the electrostatic contribution dominates and the total energy of ii drops below that of i. However, transannular electrostatic interactions may not be a dominant factor in solution because the atom charges are shielded by solvation. A distance-dependent dielectric, $\epsilon = 5R_{ij}$, was approximately the minimum dielectric value that gave a relative population of conformers that was constant and without an overemphasis of electrostatics. Similar total energies are calculated for the major conformers, i and ii, at $\epsilon = 5R_{ij}$ and $10R_{ij}$, and are consistent with the NMR data as noted above. Thus, the experimental measurements and calculated energies indicate a facile equilibrium between i and ii exists in solution.

Table VI. Calculated Time-Averaged Coupling Constants (Hz) at Various Dielectrics and Observed Couplings in CD_3OD

	R_{ij}	$2R_{ij}$	$5R_{ij}$	$10R_{ij}$	obsd in CD_3OD
J(2–3)	3.6	3.6	3.6	3.5	4.1
J(2′–3)	10.9	8.8	7.6	7.5	8.0
$J(H_b–7)$	6.5	6.6	6.9	7.0	7.2
J(9–10)	12.1	12.2	12.2	12.2	11.7
J(9–10′)	2.0	2.6	2.9	2.9	<2.5
J(12–13)	11.2	10.9	10.6	10.6	
J(13–14)	11.6	11.0	10.5	10.2	10.2
J(13–14′)	1.7	2.3	2.9	3.2	4.8
J(14–15)	2.2	3.1	4.3	4.7	5.8
J(14′–15)	9.6	9.5	8.8	8.4	8.2

Time-averaged coupling constants were calculated with eq 2, where P_i is the population of conformation i, and ^3J_i is the calculated coupling constant for conformation i. The averaged

$$^3J_{av} = \sum_i P_i {}^3J_i \quad (2)$$

coupling constants, shown in Table VI, were computed by using the relative conformer populations and couplings predicted from mechanics calculations with ϵ from R_{ij} – $10R_{ij}$. Similar energies and conformations were calculated with a distance-dependent dielectric, $\epsilon = 10R_{ij}$, or with a constant dielectric, $\epsilon = 35$. The dielectric constant of methanol is 33.6. The calculated vicinal coupling constants for **3** with $\epsilon = 10R_{ij}$ or $\epsilon = 35$ compare favorably to the couplings observed for **1** in CD_3OD; the root-mean-square deviation between the observed and calculated couplings is 0.7 Hz. The largest deviations occurred with J(13–14′) and J(14–15).

The influence of solvation on relative conformer populations is also seen in the ^3J coupling constants of **1** measured in different solvents (Table IV). The ^3J value for H14–H15 changes dramatically from 3.0 Hz in a relatively nonpolar solvent ($CDCl_3$) to 6.0/5.8 Hz in polar solvents (CD_3CN/CD_3OD). In nonpolar solvents the torsion angle is predominantly a (see Table V and discussions above) with a gauche interaction between H14–H15 ($^3J \approx 3$ Hz), whereas in polar solvents the coupling constant increases and represents a mixing of states. This observation is supported by the calculations where an increase in the dielectric results in an increase in the populations of minor conformers iii–vi having an anti relationship between H14–H15 ($^3J \approx 12$ Hz). This trend can also be seen by inspecting the calculated couplings of H14–H15 at different R_{ij} values (Table VI). At $\epsilon = R_{ij}$ the overall sum of the minor conformers, iii–vi, was 10% and this increased to 30% at $10R_{ij}$ as shown in Figure 4. An analogous situation also occurs with H13–H14. The dependence of the minimized energies of **3** on the dielectric indicates that mechanics calculations of cyclic peptides should not be done with a gas-phase dielectric if correspondence to solution-phase results is desired.

The above analysis afforded the relative weighting of the various backbone conformations of **3**. Assuming a parallel situation for **1**, it was possible to assign each of the diastereotopic hydrogens, as shown in **1**, on the basis of the relative population of each conformer and their calculated coupling constants. This strategy offers a convenient alternative to the approaches reviewed by Govil and Hosur,[33] which involve either stereoselective deuteration of one of the diasterotopic hydrogens or the simultaneous use of three-bond carbon–proton couplings between a carbonyl carbon and β-protons in which the anti and gauche coupling constants

(32) Dosen-Micovic, L.; Jermic, D.; Allinger, N. L. *J. Am. Chem. Soc.* **1983**, *105*, 1723.

(33) Reference 25b, p 97.

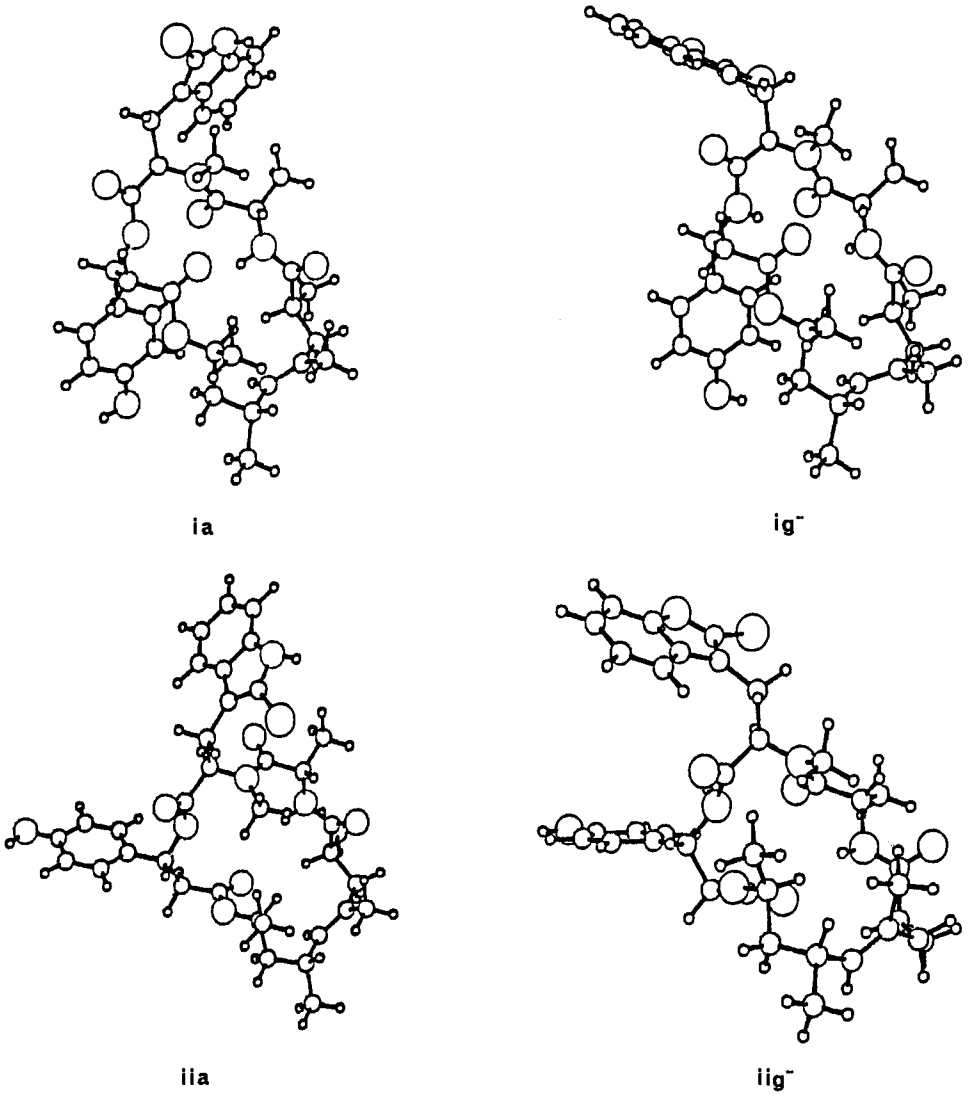

Figure 5. ORTEP plots of conformers ia, ig⁻, iia, iig⁻.

are assumed to be 11 and 1 Hz, respectively.[34]

Side-Chain Conformations. The remaining problem to be addressed concerned the relative orientations of the phenol and bromoindole side chains present in **1** but not in **3**. The major backbone conformations of i and ii were used as a starting point for calculations to estimate the bromoindole side-chain conformation. The calculations indicated that the indole may adopt either the a or g⁻ conformation about the C4–C5–C20–C21 torsion angle shown below. Four conformers are possible, which are ia, iia, ig⁻, iig⁻, and these are shown in Figure 5. The ia conformation is similar to that of the X-ray structure. Interconversion between the ia and ig⁻ states occurred during the dynamics calculations. Mechanics calculations predict all four of these conformers to be similar in energy as summarized in Table VII. Consequently, all four were used to compute the time-averaged coupling constants

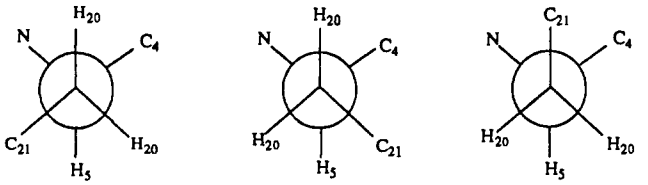

Table VII. Summary of Side-Chain Conformations for i and ii: Energies, Populations, and Calculated Time-Averaged Coupling Constants (Hz) from Molecular Mechanics Calculations ($\epsilon = 5R_{ij}$)

	conformer			
	iia	ia	iig⁻	ig⁻
rel energy, kJ/mol	0	1.1	1.5	1.9
population	0.38	0.24	0.21	0.17
J(5–20)	3.1	5.4	11.7	11.7
J(5–20′)	11.8	10.8	2.4	2.5
calcd time-averaged coupling constants:		J(5–20) = 6.9; J(5–20′) = 8.0		
obsd coupling constants (CD_3OD):		J(5–20) = 7.2; J(5–20′) = 9.3		

for J(5–20) and J(5–20′) which compare favorably to the observed values (see Table VII).

Cooperative side-chain interactions between the phenol and indole groups are possible only when the C1–C2–C3–N torsion angle is in the g⁺ state (as in ii, iii, iv, vi) and when the C4–C5–C20–C21 torsion angle occupies the g⁻ state (as in iig⁻, iiig⁻, ivg⁻, vig⁻). Side-chain interactions were explored for iig⁻ in which the indole and phenol side chains are nearly coplanar and are approximately 6–7 Å apart. In iig⁻ there are two limiting possibilities for the parallel orientations between the aromatic rings where the distance between them may vary from a molecular tweezer (MT) arrangement to a close face–face (FF) orientation. These limiting conformations, MT and FF, were examined by mechanics calculations, and the results of total energies (E_T) and partial contributions from the VDW and electrostatic (E_I) energies are shown in Table VIII. The MT conformation, shown in Figures 1 and 6, was investigated by invoking distance constraints

(34) Hansen, P. E.; Feeney, J.; Roberts, G. C. K. *J. Magn. Reson.* **1975**, *17*, 249.

Table VIII. Energetics of Side-Chain Orientations in iig⁻ ($\epsilon = R_{ij}$)

	E_T[a]	VDW[b]	E_l[c]	H_{bond}[d]
iig⁻	−73.0	7.9	−125.5	−3.5
MT	−67.6	6.6	−120.5	−4.2
FF	−72.8	−5.9	−108.0	−3.9

[a] Total energy (kJ/mol). [b] Van der Waal's energy. [c] Electrostatic energy. [d] Hydrogen-bonding energy.

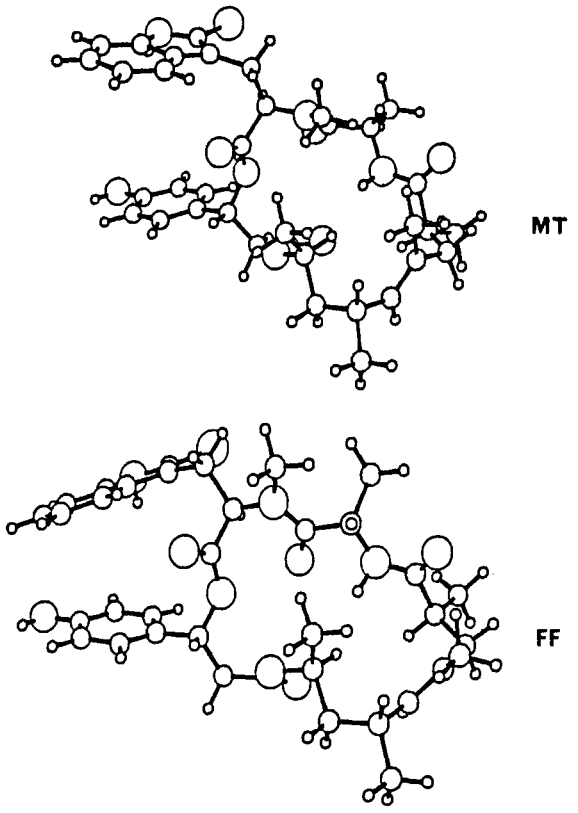

Figure 6. ORTEP plots of the molecular tweezer and face–face iig⁻ conformations.

on the aromatic side chains so that the two rings attained a coplanar geometry with approximately 6.5 Å between rings. In comparison to iig⁻ an increase of 3–5 kJ/mol was predicted for the MT state. The FF conformation, shown in Figure 6, has the VDW surfaces of the aromatic rings in contact, and the VDW energy term contributes −14 kJ/mol in energy stabilization. The total energy (E_T) for the FF conformation is approximately the same as calculated for the iig⁻ conformation. However, force field calculations do not calculate all nonbonded variables involved with this type of interaction. There is no energy term for the charge-transfer (HOMO–LUMO) interaction in the force field. In this case, both aromatic rings are electron rich and would have an unfavorable HOMO–LUMO interaction.[35] A NOE correlation between H18–H24 would be predicted for this conformation and was not observed in CD_3CN or $DMSO/D_2O$.

It is generally believed that the overall shape of a peptide is influenced by the relative orientation of amino acid side chains.[36] Thus, it is relevant to comment on how the macrocyclic backbone of jasplakinolide is influenced by the bromoindole side chain. This can be addressed by comparing the changes in conformations and relative energies obtained in the modeling results of **3** and **1**. For **3**, conformer i is more stable than ii but by only 0.5 kJ/mol (Table V), whereas the order is reversed in **1**, iia is 1.1 kJ/mol lower than ia, and iig⁻ is 0.4 kJ/mol lower than ig⁻. Since these conformations are nearly isoenergetic, it appears that the side chains have a minimal influence on the relative energies of i and ii. However, the large bromoindole side chain was found to effect the backbone conformation of ia. Minimization of sampled structures from a 300 K dynamics trajectory of ia indicated that the bromoindole may also adopt a closer position to the NCH_3, causing the NCH_3 to rotate toward the macrocycle plane, thus forcing the C1 carbonyl of the β-tyrosine to rotate below the plane of the macrocycle. Interestingly, the two conformations of ia were nearly isoenergetic and had similar calculated coupling constants. Large torsional variations between the two ia conformations were calculated to occur about the C14–C15–O–C1 and the O–C1–C2–C3 torsion angles and suggest how the flexible β-tyrosine may adjust to steric impositions.

Conclusions

Analysis of molecular modeling and NMR results indicates the backbone conformation of **1** in solution, as estimated by modeling studies on **3**, is comprised of six conformers (i–vi). The two major backbone conformers of **3** (or **1**) are i (or ia/ig⁻) and ii (or iia/iig⁻), which differ by ≈120° rotation at the C1–C2–C3–N torsion angle within the β-tyrosine. Additional backbone flexibility was noted in the C12–C13–C14–C15 and C13–C14–C15–O torsion angles within the tetrapropionate group. The relative populations of the six backbone conformers were dependent on the dielectric term used in the force field and reflect the effect of solvation. The relative populations of the minor conformers (iii, iv, v, vi) predicted by mechanics calculations increased from 10% with $\epsilon = R_{ij}$ to 30% with $\epsilon = 10R_{ij}$, and this general trend was also observed in the J values of **1** measured in solvents of varying polarity. The backbone and side-chain conformations of **1** may play an important role in molecular recognition. We are currently investigating this possibility in terms of the ability of conjugated π-systems to bind between the aromatic side chains of the iig⁻-type conformation and the ability of cations to bind to the cavity present in i and ii.

Some preliminary insights into the conformation of **2** may now be discussed with an understanding of the conformational properties of **1**. In contrast to **1**, the NMR data of the **2** in CD_3OD or CD_3CN suggests the C1–C2–C3–N torsion angle is predominately in either the g^+ or a conformation. This is based on the relatively large chemical shift difference between H2 and H2′ diastereotopic hydrogens (0.38 ppm) and the extreme difference in ^3J values for H2–H3 (10.5 Hz) and H2′–H3 (3.1 Hz). We are currently carrying out conformational analyses of the 9-epimethyl isomer and other appropriate analogues, especially the geodiamolides,[6] in an effort to construct a model for their biological activity.

Acknowledgment. Partial research support was from a NOAA, National Sea Grant College Program, Department of Commerce, University of California project no. R/MP-41, a grant from the Research Corp., and a grant from UC Santa Cruz Committee on Research. The U.S. Government is authorized to produce and distribute reprints for governmental purposes. We thank Professor Paul Grieco (University of Indiana) for providing compound **2**. We are appreciative for Dr. Clark Still (Columbia University) for providing a copy of MACROMODEL (version 1.5) and to Dr. Robert McDowell for advice in the use of this program.

(35) The HOMO/LUMO (eV) energies were calculated by use of MINDO3 and are as follows: 4-methylphenol −8.3/1.1; 2-methylindole −7.8/0.92.

(36) For example, see: Kessler, H.; Griesinger, C.; Wagner, K. *J. Am. Chem. Soc.* **1987**, *109*, 6927.